International Journal of Nanomedicine

Dovepress
open access to scientific and medical research

Open Access Full Text Article

ORIGINAL RESEARCH

Pilot study on biocompatibility of fluorescent nanodiamond-(NV)-Z~800 particles in rats: safety, pharmacokinetics, and bio-distribution (part III)

This article was published in the following Dove Press journal:
International Journal of Nanomedicine

Frank C Barone[1]
Cezary Marcinkiewicz[2,3]
Jie Li[1]
Mark Sternberg[3]
Peter I Lelkes[2]
Dmitriy A Dikin[4]
Peter J Bergold[1]
Jonathan A Gerstenhaber[2]
Giora Feuerstein[3]

[1]Department of Neurology, SUNY Downstate Medical Center, Brooklyn, NY, USA; [2]Department of Bioengineering, Temple University, College of Engineering, Philadelphia, PA, USA; [3]Debina Diagnostics Inc, Newtown Square, PA, USA; [4]Department of Mechanical Engineering, Temple University, Philadelphia, PA, USA

Introduction: We hereby report on studies aimed to characterize safety, pharmacokinetics, and bio-distribution of fluorescent nanodiamond particles (NV)-Z~800 (FNDP-(NV)) administered to rats by intravenous infusion in a single high dose.

Methods: Broad scale biological variables were monitored following acute (90 minutes) and subacute (5 or 14 days) exposure to FNDP-(NV). Primary endpoints included morbidity and mortality, while secondary endpoints focused on hematology and clinical biochemistry biomarkers. Particle distribution (liver, spleen, lung, heart, and kidney) was assessed by whole organ near infrared imaging using an in vivo imaging system. This was validated by the quantification of particles extracted from the same organs and visualized by fluorescent and scanning electron microscopy. FNDP-(NV)-treated rats showed no change in morbidity or mortality and preserved normal motor and sensory function, as assessed by six different tests.

Results: Blood cell counts and plasma biochemistry remained normal. The particles were principally distributed in the liver and spleen. The liver particle load accounted for 51%, 24%, and 18% at 90 minutes, 5 days, and 14 days, respectively. A pilot study of particle clearance from blood indicated 50% clearance 33 minutes following the end of particle infusion.

Conclusion: We concluded that systemic exposure of rats to a single high dose of FDNP-(NV)-Z~800 (60 mg/kg) appeared to be safe and well tolerated over at least 2 weeks. These data suggest that FNDP-(NV) should proceed to preclinical development in the near future.

Keywords: fluorescent nanodiamond particles, biocompatibility, near infrared imaging, scanning electron microscopy, neurobehavioral function, pharmacokinetics, rat

Introduction

Recent years have ushered in a strong and growing interest in the bioengineering of nanodiamond particles (NDP).[1–5] Certain strains of NDP, such as the fluorescent NDP (FNDP), have been prospected for multiple medical diagnostic tests, drug delivery vehicles, imaging biomarkers, cell tracking, and translational biomarkers.[6–10] The highly diverse options available for chemical modifications of NDP enable co-junction with materials that offer opportunities for imaging targeted pathologies such as tumors[11,12] or blood clots.[13] NDP are also being extensively studied as carriers of pharmacological agents for delivery of cytotoxic chemicals into drug-resistant tumors.[14–17] Furthermore, new frontiers were recently broached that demonstrate potential medical application in immune enhancement (vaccine),[18,19] adjuvant,[20] and genetic neurological conditions.[21] Pharmacokinetic (PK) advantages gained by the co-junction of tumor-toxic compounds to NDP have shown preservation of efficacy

Correspondence: Cezary Marcinkiewicz
Department of Bioengineering, Temple University, College of Engineering, 1947 N 12th St, Philadelphia, PA 19122, USA
Tel +1 215 204 3307
Email cmarcink@temple.edu

submit your manuscript | www.dovepress.com
Dovepress
http://dx.doi.org/10.2147/IJN.S171117

while reducing the compounds' toxicity by restriction of the dosing regimen.[22] However, although NDP research holds promising medical opportunities, it is still largely an experimental and preclinical research endeavor.

More recent manipulations at the atomic crystal structure level of NDP yielded "color centers" that can emit bright fluorescence, for example, NV centers, which fluoresce in the near infrared (NIR) and are resistant to photo-bleaching.[23,24] We recently reported on a 800-nm strain of bioengineered particles (FNDP-(NV)-Z~800) ligated with the disintegrin protein bitistatin (Bit). This construct should enable association of the fluorescent particles with activated platelets known to comprise the principal cellular component of blood clots. Such NIR fluorescence may enable light-based assessment of thrombus characteristics and distribution in an ambulatory setting. FNDP-(NV)-Z~800/Bit enables efficient binding to the isolated human platelet fibrinogen receptor (αIIbβ3 integrin) as well as to platelet-rich plasma clots in vitro.[13] We subsequently tested and confirmed the association of FNDP-(NV)/Bit constructs with acutely formed vascular blood clots in the carotid bifurcation of anesthetized rats.[25] In the latter study, extracorporeal imaging of blood clots in the carotid artery bifurcation was demonstrated by monitoring NIR light emission using an in vivo imaging system (IVIS). These studies were made possible by the exceptional optical properties of FNDP-(NV), which emit strong NIR light in response to excitation that could not be monitored with an earlier brand of FNDP-(NV).[25]

Our recent work therefore suggests that bioengineered FNDP-(NV)/Bit could assist in vascular blood clot imaging in humans using extracorporeal devices following minimally invasive procedures, such as a brief, single systemic intravenous (IV) injection of FNDP-(NV). Such an imaging technology could be of particular importance in the diagnosis of high risk blood clots as part of a management strategy to mitigate thromboembolic events (TEE), resulting in cardiovascular morbidity and mortality (eg, strokes and heart attacks).

In light of the prospect to achieve extracorporeal vascular (blood clots) imaging based on NIR emission from FNDP-(NV) incorporated within blood clots, we embarked on pilot/exploratory safety studies in rodents using a non-good laboratory practice (GLP) format. This study provides original data that characterize safety, PKs, and selected organ distribution of FNDP-(NV)-Z~800 in rats. We chose to deploy IV particle dosing simulating the intended application in humans. We used a dosing regimen in excess of that used in our recent in vivo "proof of concept" (POC) studies to broaden the therapeutic index.[23] The tactical approach is built on a tier (ie, adaptive) design exploring acute (90 minutes) and subacute (5 or 14 days) protocols. Broad scale biological variables including morbidity and mortality, organ particle distribution (liver, spleen, kidney, lung, and heart), as well as blood biomarkers were monitored. We deployed several independent, yet complementary methods to monitor the presence of particles in organs including three NIR light emission techniques and direct scanning electron microscopy (SEM) imaging. In addition, a PK study aimed to define clearance dynamics of FNDP-(NV) in the acute postexposure period was performed. We consider our pilot studies to be translational guidance toward formal GLP preclinical development needed for an investigational new drug (IND) application.

Materials and methods

Nanoparticles source and processing

FNDP with NV "color centers" (FNDP-(NV)), chemically surface-functionalized with carboxyl groups (–COOH), were purchased from ADAMAS Nanotechnologies (Raleigh, NC, USA). FNDP-(NV) were sterilized by immersion with 70% ethanol for 15 minutes at room temperature, as previously described. Sterility of FNDP-(NV) was vetted by standard laboratory methods for lack of bacterial growth. FNDP-(NV) were incubated with 3% BSA (Sigma-Aldrich, St Louis, MO, USA) in PBS for 1 hour at 37°C to block nonspecific binding. BSA-treated FNDP-(NV) had a similar Z-average diameter as the non-blocked FNDP-(NV) (858±47 vs 817±21 nm, P=0.46, Figure S1). BSA-blocked FNDP-(NV) had a negative zeta potential of −56 mV (data generated by ADAMAS Nanotechnologies).

Animal source and husbandry

All animal procedures were performed according to the guidelines of the US Animal Welfare Act and approved by the Institutional Animal Care and Use Committee at SUNY Downstate Medical Center, NYC (Association for Assessment and Accreditation of Laboratory Animal Care International accredited). Adult male Sprague Dawley rats (350%±10% g of body weight; Charles River Laboratories, Wilmington, MA, USA) were maintained on a 12 hours light dark cycle and had ad libitum access to standard lab chow and tap water.

Anesthesia, surgery, and protocol design

The animals were anesthetized using 4% isoflurane (IF) for induction followed by 1%–2% IF (maintenance) adjusted throughout the procedure. Rats were held in the supine position and subjected to surgery aided by binoculars under aseptic conditions. A PE-10 cannula was inserted into the left

femoral vein for infusion of FNDP-(NV) particles or vehicle control (PBS). The particles (60 mg/kg rat body weight) were suspended in 2 mL PBS and vortexed immediately before loading into a 5-mL syringe. The infusions (FNDP-(NV) or PBS/control) were completed over 30 minutes and then followed by 0.3 mL PBS to flush the IV line. The design of the in vivo studies is illustrated in Figure 1.

Organ preservation

Upon completion of the in vivo protocol (90 minutes, 5 days, or 14 days), rats were anesthetized with 5% IF for deep hypnosis, and the abdominal aorta was quickly isolated and cut to allow blood drainage. Thereafter, the exsanguinated animals were perfused (10 mL) with preservation solution (70% denatured ethanol) to minimize blood remaining in the organs. Organs were carefully dissected and suspended in excess 70% denatured ethanol until further processing for ex vivo NIR fluorescence evaluation, as described below.

Blood collection and processing for PKs of FNDP-(NV) in blood

Blood samples obtained from anesthetized rats injected systemically with FNDP-(NV) as described in the above protocol design were collected from the femoral vein at the time points indicated in Figure 2A in increasing volumes (0.5, 1, 1, 1, and 3 mL) to improve particle detection. Blood was immediately mixed with a 3.8% citrate solution (9:1 v/v ratio) in Eppendorf polypropylene micro-centrifuge tubes (1.5 mL; Thermo Fisher Scientific, Waltham, MA, USA) and stored refrigerated until assayed for the presence of FNDP-(NV). Anticoagulated blood was centrifuged at 16,000×*g* for 5 minutes at room temperature. Plasma was aspirated and the pellet resuspended in 1 mL of 12N HCl. The mixture was incubated overnight at 60°C to disrupt cell membranes and release all particles, which might have been absorbed by blood cells. Since residual tissue digest remaining in the particle suspension may compromise the fluorescence readout, the following centrifugal purification procedure was applied. Tubes were centrifuged again, as described earlier, and the supernatant containing a suspension of organic residues was removed by aspiration. The pellets containing FNDP-(NV) were washed by resuspension in 1 mL of distilled water. Tubes were centrifuged a final time as earlier, and FNDP-(NV) were resuspended in 0.9 mL (dilution factor for sodium citrate) of water. The isolated particle extract was stored at 4°C. Aliquots (100 µL) of this suspension were titrated in quadruplicate into a 96-well plate along with standard curve samples (see in section "Construction of standard curves" and Figure S2B). Fluorescence of the 96-well plate was measured immediately after plate preparation in a Tecan Infinite

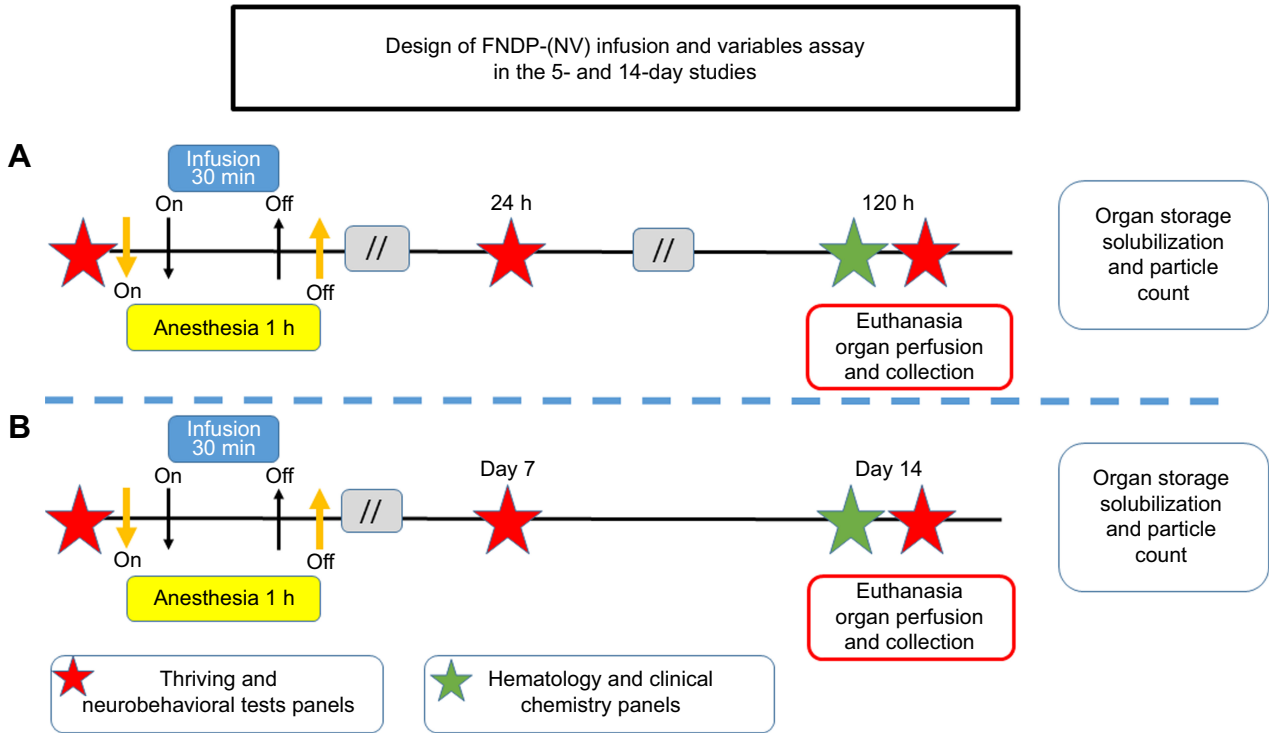

Figure 1 Design of in vivo FNDP-(NV) exposure in rats.
Note: Diagram representing (**A**) the 5-day study and (**B**) 14-day study.
Abbreviation: FNDP-(NV), fluorescence nanodiamond particles with NV active centers.

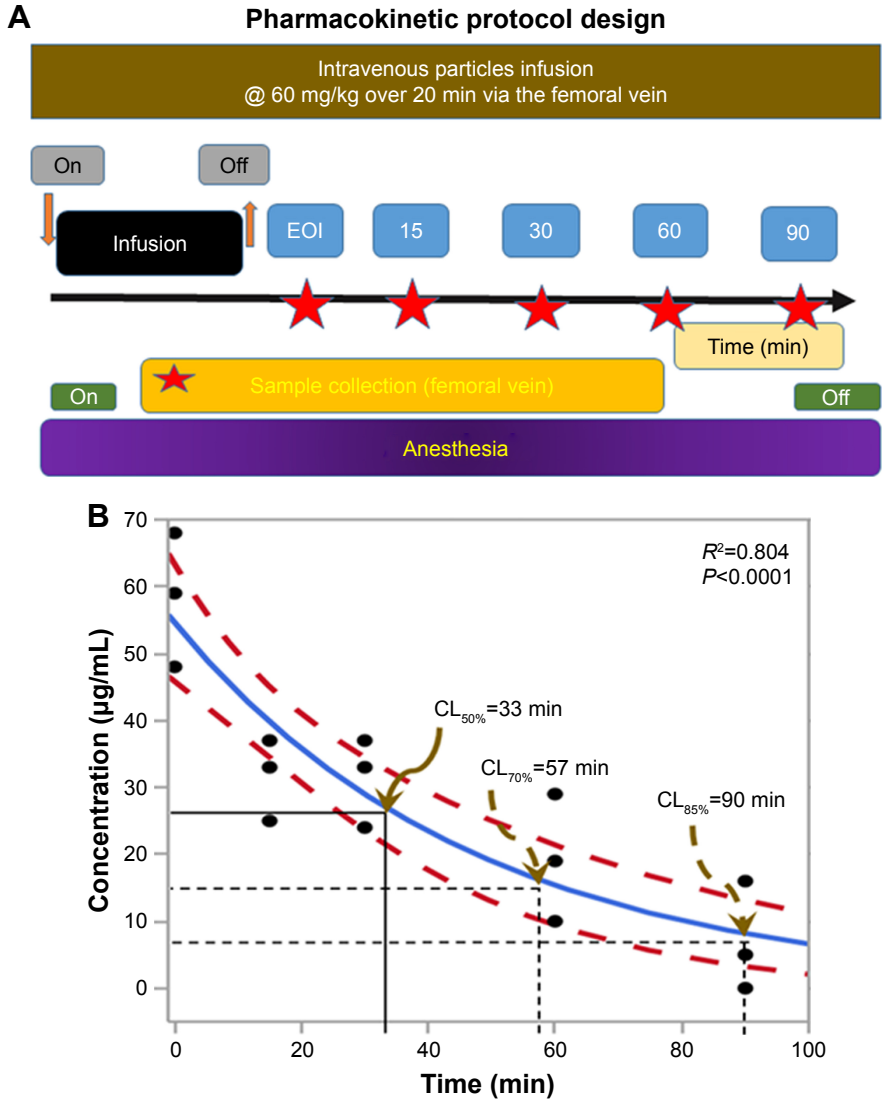

Figure 2 Blood PK studies – design and results.

Notes: (**A**) Design of the PK protocol for FNDP-(NV) infusion and blood collection. (**B**) Change of concentration of FNDP-(NV) over time. Blue line indicates mean blood particles concentration assessed by nonlinear algorithm[41] and dashed red line 95% CIs. Black solid lines represent the first calculated 50% clearance and dashed black lines the terminal 50% clearance. Brown arrows indicate various times of clearance.

Abbreviations: FNDP-(NV), fluorescence nanodiamond particles with NV active centers; CL, clearance; EOI, end of infusion; R^2, square of regression of mean data; *P*, value of statistical significance of regression analysis for nonlinear data; PK, pharmacokinetic.

200 PRO (Tecan AG, Männedorf, Switzerland) plate reader set to the appropriate wavelengths (excitation 570 nm and emission 670 nm used to detect the near IR fluorescence of FNDP-(NV)), as previously described.[13]

Ex vivo imaging of whole organs by IVIS

NIR fluorescence imaging of whole organs was carried out by IVIS (IVIS 50 Imaging System; PerkinElmer Inc, Waltham, MA, USA) using 580–610 nm for excitation and 695–770 nm for emission bandpass filters, with 5 second exposure, "binning" set to 4, and a 10-cm field of view, as reported previously.[13,25] Autofluorescence was subtracted based on excitation at 445–490 nm under otherwise identical imaging conditions. For each organ, the mean fluorescence intensity of the image, adjusted for autofluorescence, was evaluated using proprietary IVIS software. (Living Image; 4.3.1 software; Caliper Life Sciences, Hopkinton, MA, USA)

Quantification of FNDP-(NV) extracted from solubilized organs

To improve the sensitivity of FNDP-(NV) detection, particles were extracted from organ tissues in a fashion similar to the extraction protocol for blood collection. Organs were cut into 0.2–0.3 cm pieces and immersed in 12N HCl at a ratio of 0.5 g tissue/mL of 12N HCl and incubated overnight at 60°C followed by centrifugation, decanting, resuspension in

deionized water, and a final centrifugation and resuspension of the isolated particles as described earlier. Samples containing particles from solubilized organs and normalization standards (see in section "Construction of standard curves" and Figure S2A) were applied on the same 96-well plate, which was read in the Tecan plate reader, as described for blood analysis.

Construction of standard curves for particle calibration

To minimize interference from nonspecific autofluorescence originating from residual non-solubilized biological materials that might have remained in the 12N HCl digest, an additional standard curve was constructed by admixing known amounts of FNDP-(NV) to an untreated organ followed by digestion and extraction as described. For this process, we selected the liver as our model organ, since it presented a major site of the FNDP-(NV) accumulation. The efficiency of recovery of FNDP-(NV) from tissue after solubilization in 12N HCl is presented in Figure S2A in comparison with a standard curve constructed by direct suspension of FNDP-(NV) in water. Both standard curves are almost identical, suggesting that the procedure leads to negligible loss of particles for quantitative evaluation. A similar comparison of the recovery of FNDP-(NV) from whole blood is presented in Figure S2B. The curve constructed based on the suspension of FNDP-(NV) in water is also virtually identical to that constructed for the quantification of FNDP-(NV) in the blood.

Tissue sectioning and histology analysis

Histochemical analysis was performed on formalin-fixed, paraffin-embedded tissue as previously described.[26] Tissue sections (5 μm thick) prepared by microtome (RM2255; Leica Microsystems, Wetzlar, Germany) stained for actin cytoskeleton (fluorescein isothiocyanate-phalloidin), nucleus (DAPI), and potentially containing FNDP-(NV) were analyzed in a fluorescence microscope (FSX100; Olympus Corporation, Tokyo, Japan) using green, blue, and red filters, respectively, with 20× and 40× objectives.

SEM

A detailed surface morphology of FNDP-(NV) absorbed by the liver and spleen and the surrounding tissue of these organs was imaged using environmental SEM (Quanta 450FEG; FEI Co, Hillsboro, OR, USA) operated in the low vacuum mode at 0.3–0.4 Torr of water vapor pressure and 7–10 keV of acceleration voltage. Tissue samples were de-paraffinized in xylene. Sections (5 μm thick) were fixed onto glass slides without any additional treatment or coatings. Since the concentration of FNDP-(NV) in the tissues was relatively low, we searched for the particles by simultaneously employing the secondary electron and the backscattered electron detectors. SEM imaging was performed in the College of Engineering, Nano Instrumentation Center facility at Temple University, Philadelphia, PA, USA.

Neurobehavioral tests

Sensory motor/neurological and cognitive performance was measured as described previously.[27,28] Tests were performed prior to infusion and then over 5 or 14 days. Sensory motor tests were scored individually and according to the modified neurologic function severity score (mNSS). The data from each individual test and the total score calculated from individual tests that make up the mNSS were measured. Active place avoidance learning performance, a complex cognitive assay very sensitive to brain injury that measures the ability of rats to avoid negative reinforcement on a rotating arena, was also measured. Detailed results are provided in Table S1.

Beam balance test

Rats were placed on a 1-inch wide beam for 60 seconds. A normal response is balance with steady posture for 60 seconds (a score of 0). Deficits are scored if the rat: grasps the side of the beam (a score of 1), hugs the beam and one limb falls down from the beam (a score of 2), hugs the beam and two limbs fall off the beam (a score of 3), attempts to balance on the beam, but falls off from 40±59 seconds (a score of 4), attempts to balance on the beam but falls off from 20±39 seconds (a score of 5), or falls off with no attempt to balance or hang on the beam in <20 seconds (a score of 6).

Foot fault test

Forelimb movement dysfunction, while walking on elevated metal grids, was monitored. The animal was placed on horizontal grids (85.5×26.5×20) cm with a glass enclosure for observation. With each weight bearing step, the forelimb can fall or slip between the metal support bars, an event recorded as a foot fault. The total number of forelimb steps and the total number of foot faults are recorded. The percentage of forelimb foot faults to the total steps that occurred within 2 minutes marks the test results.

Hind limb placing test

This proprioceptive test monitors reposition of hind limbs placed down and away from the table edge. The ability to retrieve and place the hind limbs back onto the table was scored. Immediate and complete limb retrieval was scored 0, delayed (>2 seconds) limb retrieval and/or interspersed flailing was scored 1, and no limb retrieval was scored 2.

Increasing platform angle to slide test

This test monitors the strength and stability of resistance to slide down an inclined platform. It deploys a clean wooden board (66 cm by 44 cm) positioned horizontally. Rats are placed on the board with head facing up the increasing incline. The board then swings to increase the degree of inclination the rat experiences until slipping down the board feet first. The degree of the angle at which the rat relinquishes their grip/stance on the board (slips down) constitutes the test results.

The forelimb whole body suspension test

The test measures grip strength by duration of suspension by forepaws. The rat is suspended on a metal bar (diameter 5 mm) which it tightly holds onto by its forelimbs. The time (seconds) during which each rat could sustain its weight while holding onto the bar (32 inches from the floor) is recorded. Rats drop from the bar onto soft material with no harm. The test was repeated three times and a mean result per rat was used as the score.

Hematology and biochemistry tests

Blood was collected at the endpoints of the respective experiments (5 and 14 days) by cardiac puncture under deep anesthesia and analyzed for routine blood hematology and biochemistry. The assays were performed by standard methods at SUNY Medical Center Clinical Laboratory (Brooklyn, NY, USA).

Statistical analysis

Data are presented as mean±SD. Statistical analyses were done by ANOVA (where appropriate) and Student's *t*-test (one or two tailed as noted) using SigmaPlot software (SigmaPlot® 12 SPSS; Systat Software Inc, San Jose, CA, USA). Statistical significance was established at $P<0.05$; N value indicates the number of independent animals tested.

Results

General considerations of the study design

Figure 1 depicts the key features of the experimental design of the in vivo safety studies. The 5-day format was designed as an exploratory/pilot study aimed at assessing key morbidity and mortality risks as well as the technical feasibility of data collection for the diverse variables examined. This approach was desirable, given the lack of in vivo data using FNDP-(NV)-Z~800 nm, and a regimen that calls for a single high dose can be used to possibly define the maximum tolerated dose (MTD). This approach limits the use of animals and resources should severe adverse effects require abandonment or fundamental changes in the experimental design. The follow-up studies (14 day subacute and 90 minutes PK) took advantage of the initial exploratory step, which warranted increased duration and depth of investigation of particle distributions at the macro and microlevels.

Effects of FNDP-(NV) on body and organ weights

Figure 3 provides body and organ weights used as indicators of the animals' thriving post particle exposure. Neither the total body weight nor the weights of individual organs of rats exposed to the particles differed from those in the vehicle control group (PBS infusion). For both 5- and 14-day experiments, visual inspection of the organ surfaces failed to identify necrosis, hemorrhages, or gross contour (fibrotic) changes (data not shown).

Effects of FNDP-(NV) on sensory motor and cognitive tests

The purpose of this set of tests was to assess integrated sensory and motor functions in awake, freely moving rats.[27,28] The data presented in Table S1 include the "raw data" to show consistency across the cohorts. In brief, treatment of rats with FNDP-(NV) had no effect on rat sensory motor or cognitive performance in any of these tests in either the 5- or 14-day protocols compared with baseline (prior to infusion of the particles) or in comparison with the vehicle control group.

Effects of FNDP-(NV) on blood cell counts and biochemical biomarkers

As seen in Figure 4, there were no differences in any of the variables tested between particle-exposed rats and rats that received vehicle controls (PBS) in either the 5- or 14-day protocols. Biochemical biomarkers of liver function (eg, aspartate aminotransferase, alanine transaminase, albumin, alkaline phosphatase) and renal function (creatinine, blood urea nitrogen) remained unchanged.

NIR fluorescence scans of whole organs by IVIS

Imaging on the IVIS system revealed robust NIR fluorescence emission from the livers and spleens collected from the 90-minute, 5-day, or 14-day protocols (Figures 5 and S3), compared with control tissue. Fluorescence background signal in the tissue can be sensitive to procedure variables;

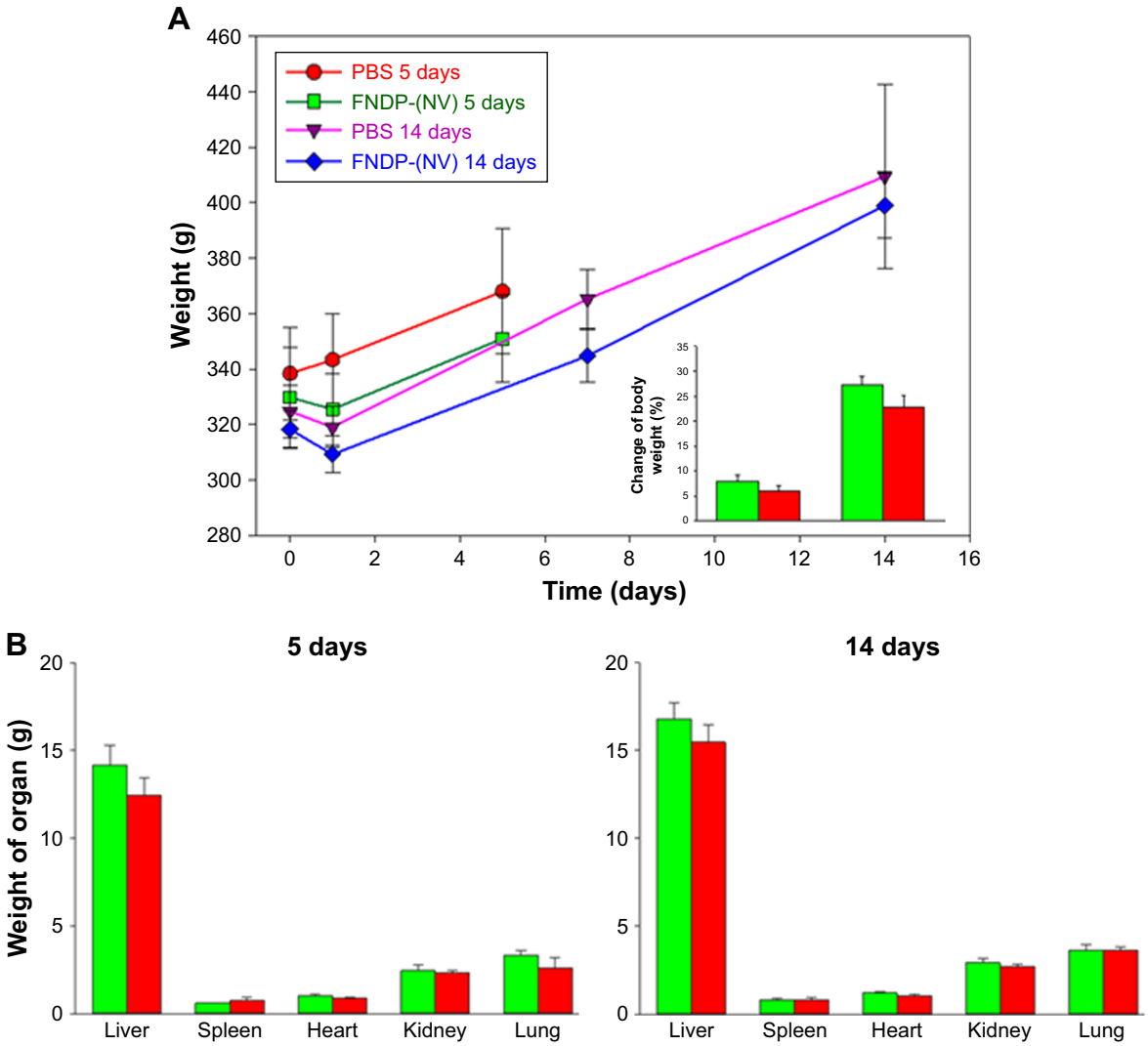

Figure 3 Comparison of body and organ weights for rats investigated in 5- and 14-day studies.
Notes: (**A**) Comparison of body weights of rats in the progression time of experiments. Inset represents the percentage of final change from baseline body weight. (**B**) Comparison of organs weight isolated on day 5 or 14 postexposure. Green bars or red bars represent vehicle control (PBS) or FNDP-(NV)-treated animals, respectively. Error bars represent SD for the 5-day control group (N=3), 5-day FNDP-(NV) group (N=4), and 14-day groups (N=4). There was no significant difference between the control and FNDP-(NV) groups ($P>0.05$ for two-tailed Student's *t*-test).
Abbreviations: FNDP-(NV), fluorescence nanodiamond particles with NV active centers; N, number of animals per group.

a comparison is best made with the respective control tissue as it is prepared directly in parallel. However, there were no significant signals over the background in the lungs, kidneys, and hearts (Figure S3).

NIR fluorescence scans of extracted particles from solubilized organs

Improved quantitative analysis of organ particle burden was accomplished through analysis of NIR fluorescence of FNDP-(NV)-Z~800 extracted from the tissue (through acid treatment, centrifugal separation, and water washing) measured in a Tecan plate reader. Analysis of the extracts from solubilized organs verified the IVIS-based estimates and further quantified the presence of FNDP-(NV) particles in both the liver and spleen (Figure 6). By contrast, no signals were detected by this method from the heart, lung, and kidney. The particle extraction analysis indicated that the bulk of injected FNDP-(NV) accumulated in the liver even after normalization by organ weight. Based on the quantitative analysis of particles derived from the solubilized organs, the total amount of particles in the liver calculated as percentage of the total dose infused amounted to 55.1%±3.1% after 90 minutes, 24.0%±2.2% after 5 days, and 18.8%±3.6% after 14 days. The difference in the amounts of particles in the liver between the 5- and 14-day groups is statistically significant by one tail ($P<0.05$) and borderline ($P=0.051$) significant

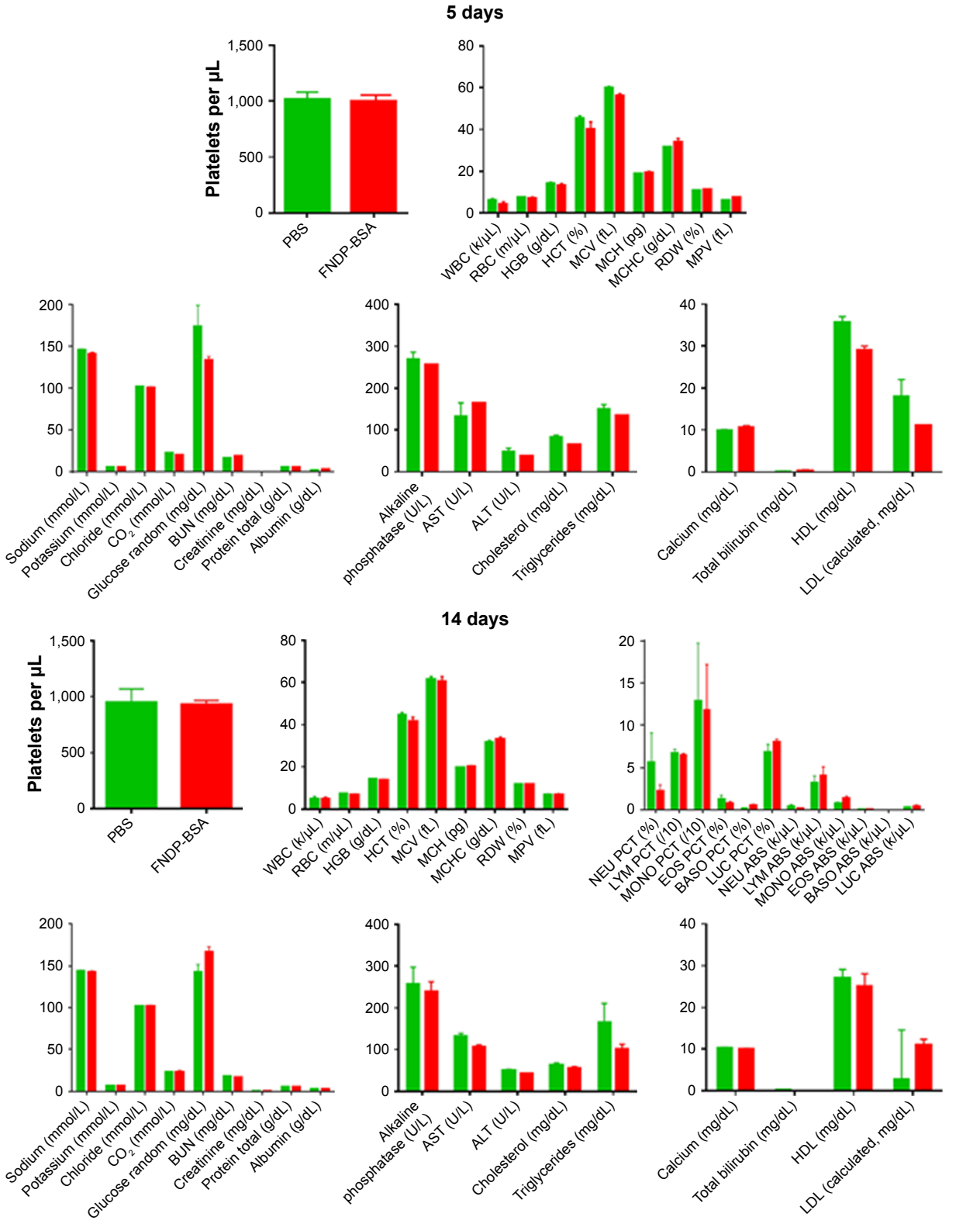

Figure 4 Blood parameters analysis of rats for 5- and 14-day studies.

Notes: Green and red bars represent vehicle control and treated particles, respectively. No statistical significance was observed between control (PBS) and FNDP-(NV)-treated groups of animals (two-tailed Student's *t*-test, $P>0.05$).

Abbreviations: FNDP-(NV), fluorescence nanodiamond particles with NV active centers; WBC, white blood cells; RBC, red blood cells; HGB, hemoglobin; HTC, hematocrit; MCV, mean corpuscular volume; MCH, mean corpuscular hemoglobin; MCHC, mean corpuscular hemoglobin concentration; RDW, red cell distribution width; MPV, mean platelet volume; NEU PCT, neutrophil percentage; LYM PCT, lymphocyte percentage; MONO PCT, monocyte percentage; EOS PCT, eosinophil percentage; BASO PCT, basophil percentage; LUC PCT, large unstained cells percentage; NEU ABS, absolute neutrophil count; LYM ABS, absolute lymphocyte count; MONO ABS, absolute monocyte count; EOS ABS, absolute eosinophil count; BASO ABS, absolute basophil count; LUC ABS, absolute large unstained cells count; BUN, blood urea nitrogen; AST, aspartate aminotransferase; ALT, alanine transaminase; HDL, high-density lipoprotein; LDL, low-density lipoprotein.

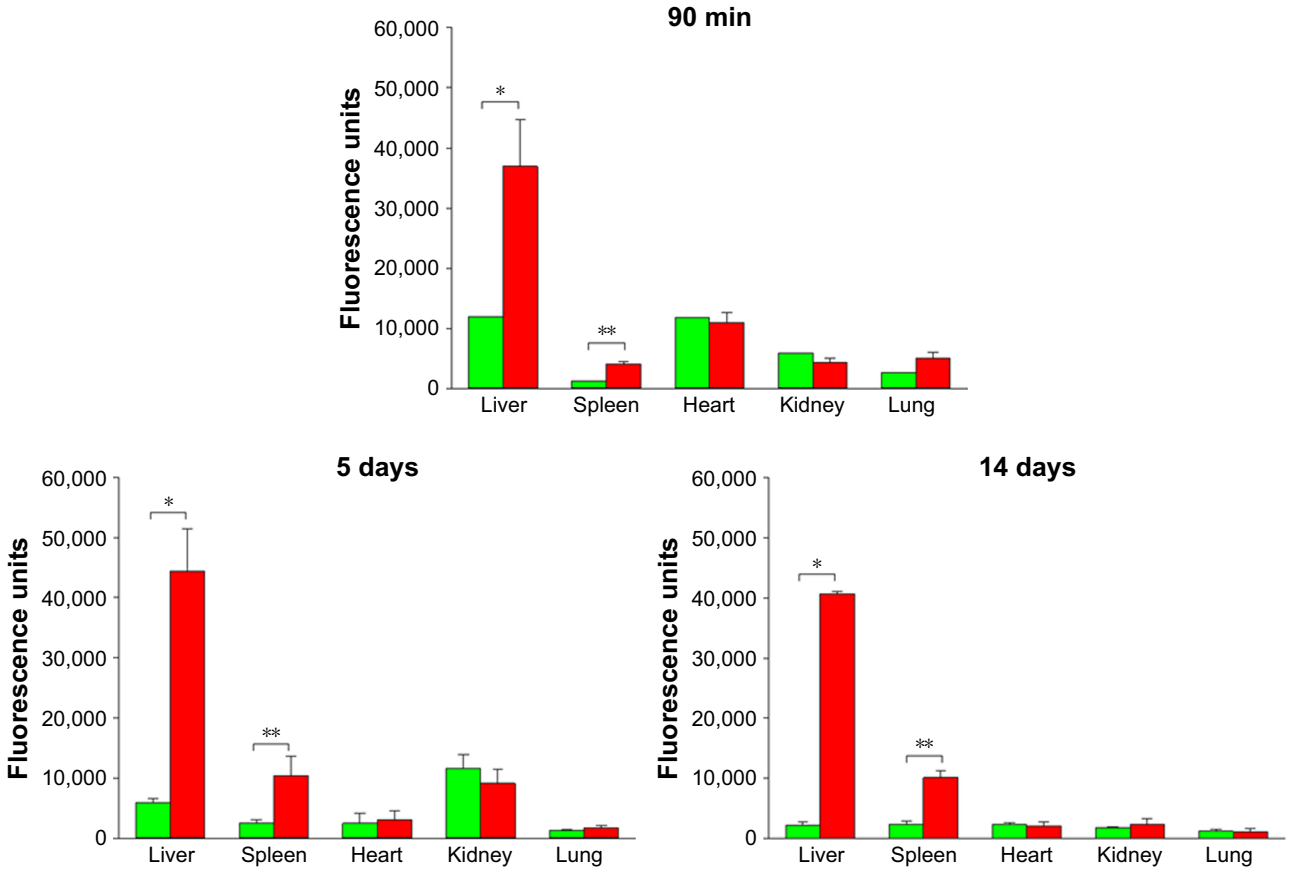

Figure 5 Comparison of fluorescence intensity of whole isolated organs in 90-minute, 5-day, and 14-day studies, obtained by measurements in IVIS instrument.
Notes: Green bars represent animals injected with vehicle control (PBS) and red bars represent FNDP-(NV)-treated rats. Error bars represent SD for N=3 for the FNDP-(NV)-treated group in the 90-minute study and N=4 for treated and control groups in 5- and 14-day studies; a single rat (N=1) was used in control for the 90-minute study (no error bars). *$P<0.001$; **$P<0.01$ compared to the control group by the two-tailed Student's *t*-test.
Abbreviations: FNDP-(NV), fluorescence nanodiamond particles with NV active centers; IVIS, in vivo imaging system; N, number of animals per group.

by the two-tailed *t*-test analysis. The difference between the particle burden in the liver in the 90-minute study is significantly different (at $P<0.001$) from that in the 5- or 14-day studies. The particle load in the spleen, when calculated per gram tissue, amounted to ~75% of that observed in the liver (Figure 6).

Fluorescent microscopy of liver and spleen histologic sections

In order to visualize the discrete (cellular level) localization of FNDP-(NV) in the organs, 5-µm sections of those tissues were imaged by fluorescent microscopy. FNDP-(NV) were visualized by NIR fluorescence in the red channel, and the blue and green channels displayed nuclei and the cytoskeleton, respectively. As shown in Figure 7, liver sections were found to contain particles in what appeared to be portal vein sinusoids and, possibly, within parenchymal cells. In the spleen, particles resided preferentially in the "red pulp" over the "white pulp" (Figure 7). The particles residing in the "red pulp" zone (where lymphocytes are more differentiated and the cytosol more developed) appeared yellow over the phalloidin green staining of the cytoskeleton, while in the "white pulp", where germinating lymphocytes are nascent (little or no "green" background), the particles appeared in the red channel only. Imaging of tissue sections from control (PBS treated) animals revealed no fluorescence signal pertinent to FNDP-(NV) (Figure S4).

NIR fluorescence microscopy of heart, lung, kidney

We considered the possibility that even though the IVIS and Tecan measurements of particles in the kidney, lung, and heart were "negative", particles might still be present at levels too low to be detected by these methods. Careful inspection of histology sections from lungs, hearts, and kidneys, that is, organs that did not generate specific NIR emission in whole organ (IVIS) or tissue extract (Tecan) in the 14-day study, failed to demonstrate the presence of particles in any of these organs. A negligible number of particles was spotted in the lung and kidney (Figure S5). Overall, although these organs cannot be

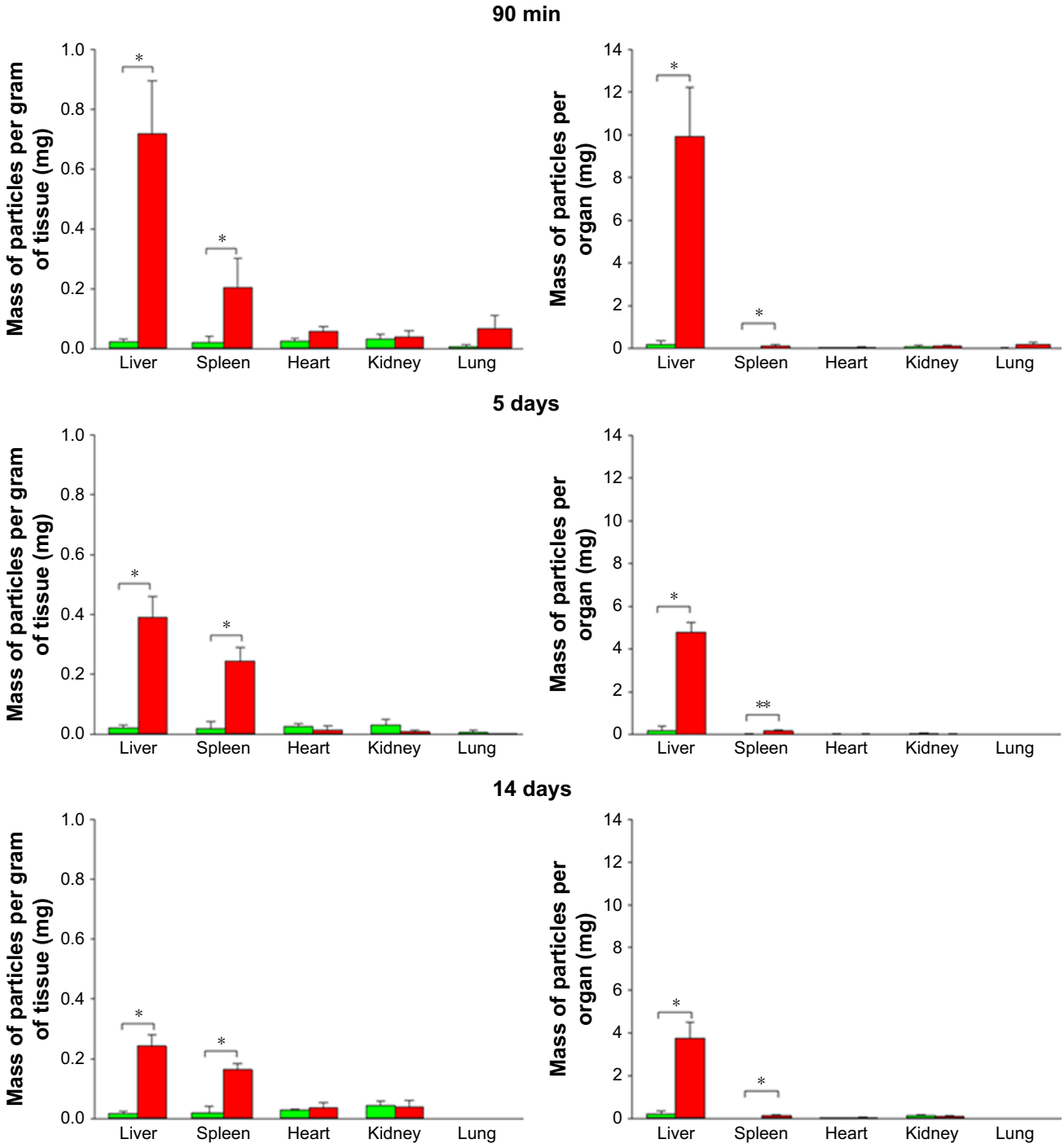

Figure 6 Comparison of FNDP-(NV) quantities assessed in solubilized organs collected from the 90-minute, 5-day, and 14-day studies.
Notes: Green and red bars represent vehicle (PBS) and FNDP-(NV)-exposed rats, respectively. Left panels represent FNDP-(NV) stratified per gram of organ weight; right panels represent total FNDP-(NV) in the whole organ. Error bars represent SD for N=8 (control group), N=3 (FNDP-(NV)-treated group for 90-minute study), and N=4 (FNDP-(NV)-treated groups for 5- and 14-day studies). *$P<0.001$; **$P<0.003$ compared to the control group by the two-tailed Student's *t*-test.
Abbreviations: FNDP-(NV), fluorescence nanodiamond particles with NV active centers; N, number of animals per group.

declared a "particle-free zone," we noted very low particle abundance, in marked contrast to the liver and spleen.

SEM of liver and spleen

We used three independent techniques to detect the presence of particles within the selected organs. All of these techniques assess a proxy marker of the particles, that is, NIR fluorescence in lieu of detecting the particles proper. Therefore, 5-µm thick tissue sections from the liver and spleen were scanned by SEM in order to directly visualize the particles accumulated in these tissues. SEM images of the particles before injection into the rats are presented in Figure 8A,

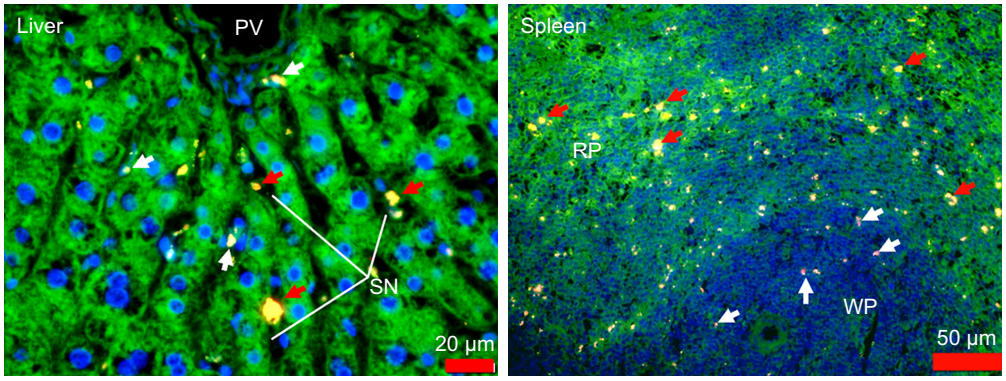

Figure 7 Fluorescence microscope images of paraffin sections of liver and spleen of rats treated with FNDP-(NV), collected on postinjection day 14.
Notes: Tissue slides were stained with FITC-phalloidin (green) and DAPI (blue). FNDP-(NV) are in yellow/red. Images were taken under a fluorescence microscope (Olympus FSX100) with 400× magnification for liver and 200× for spleen. Red arrows in the liver image indicate localization of FNDP-(NV) in sinusoids; white arrows indicate internalized FNDP into cells. Red arrows in the spleen image indicate FNDP-(NV) absorbed by the red pulp, white arrows in white pulp.
Abbreviations: FNDP-(NV), fluorescence nanodiamond particles with NV active centers; PV, portal vein; SN, sinusoids; RP, red pulp; WP, white pulp; FITC, fluorescein isothiocyanate.

suggesting that the average particle sizes closely match those obtained from dynamic light scattering (DLS; Figure S1), although the irregularly shaped particles often demonstrate dimensions below DLS estimates. SEM images of tissue sections obtained from FNDP-(NV)-treated rats revealed particles (identified by geometric similarity to the crude particle sample in Figure 8A) residing inside both organs (Figure 8B) as both individuals and small aggregates. The FNDP-(NV) appear imbedded within the tissue and there are no visible traces of their ripping out of the tissue during the process of microtome sectioning. Images of the control tissue obtained from PBS-treated animals are presented in Figure 8C.

PKs of FNDP-(NV) in blood

The experimental design of the PK studies is depicted in Figure 2A. To preserve consistency of the treatment regimen across all safety studies, that is, dose and duration of infusion, we maintained the same dosing regimen in the PK study (60 mg/kg infused over 30 minutes). Furthermore, we foresee extended infusion as a likely appropriate protocol for intended human use, though this procedure may obscure analysis of the maximum blood concentration during infusion (C_{max}). This protocol yielded a 50% mean residency following the end of infusion of 20 minutes (Figure 2B).

Discussion

The incentive for the investigation described in this manuscript stems from our recent in vivo studies on the association of FNDP-(NV)/Bit with induced vascular blood clots in the rat carotid artery bifurcation as monitored by extracorporeal NIR fluorescence.[25] In that study, the co-localization of FNDP-(NV)/Bit with blood clots was validated by three independent methods: 1) in situ extracorporeal invasive imaging (IVIS); 2) fluorescent microscopic localization by NIR imaging of isolated vessels bearing blood clots; and 3) quantitative measurement of NIR fluorescence emanating from FNDP-(NV) extracted from isolated solubilized blood clots. Taken together, our recent data[13,25] offered a "POC" that NIR emitted by FNDP-(NV) associated with vascular blood clots can serve as a surrogate biomarker for the diagnosis of blood clots by an extracorporeal method.

Since the intended use of bioengineered FNDP-(NV)/Bit would require an invasive step of IV infusion of the particles, we embarked on safety studies using canonical preclinical development tests in the same species (rat) where clot imaging has been established.[25] We have deliberately chosen a dosing regimen that exceeded that which was used in the in vivo POC studies,[25] yet is still perceived to be below the MTD. The non-GLP pilot studies described here aimed to guide the preclinical plan in lieu of expected regulatory requirements that will command GLP practices – a lengthy and costly endeavor with large-scale animal use. Our design therefore provides a "pilot investigation" as a prelude to GLP-based preclinical IND qualification studies in line with other reports using NDP.[29–32]

General conclusions from the results of these experiments are as follows: 1) no mortality was registered in any of the animals exposed to a high dose (60 mg/kg) of FNDP-(NV); 2) animals thrived well and matched the vehicle controls in terms of body and organ weight and gross appearance (Figure 3A and B); 3) blood cell counts and "clinical" biochemistry (including liver and renal functions tests) remained normal for the species (Figure 4); 4) all motor/sensory function tests were normal supporting the lack of neurological impairment (Table S1). Taken together, no severe adverse events were noted up to 14 days after the 60 mg/kg dose infusion.

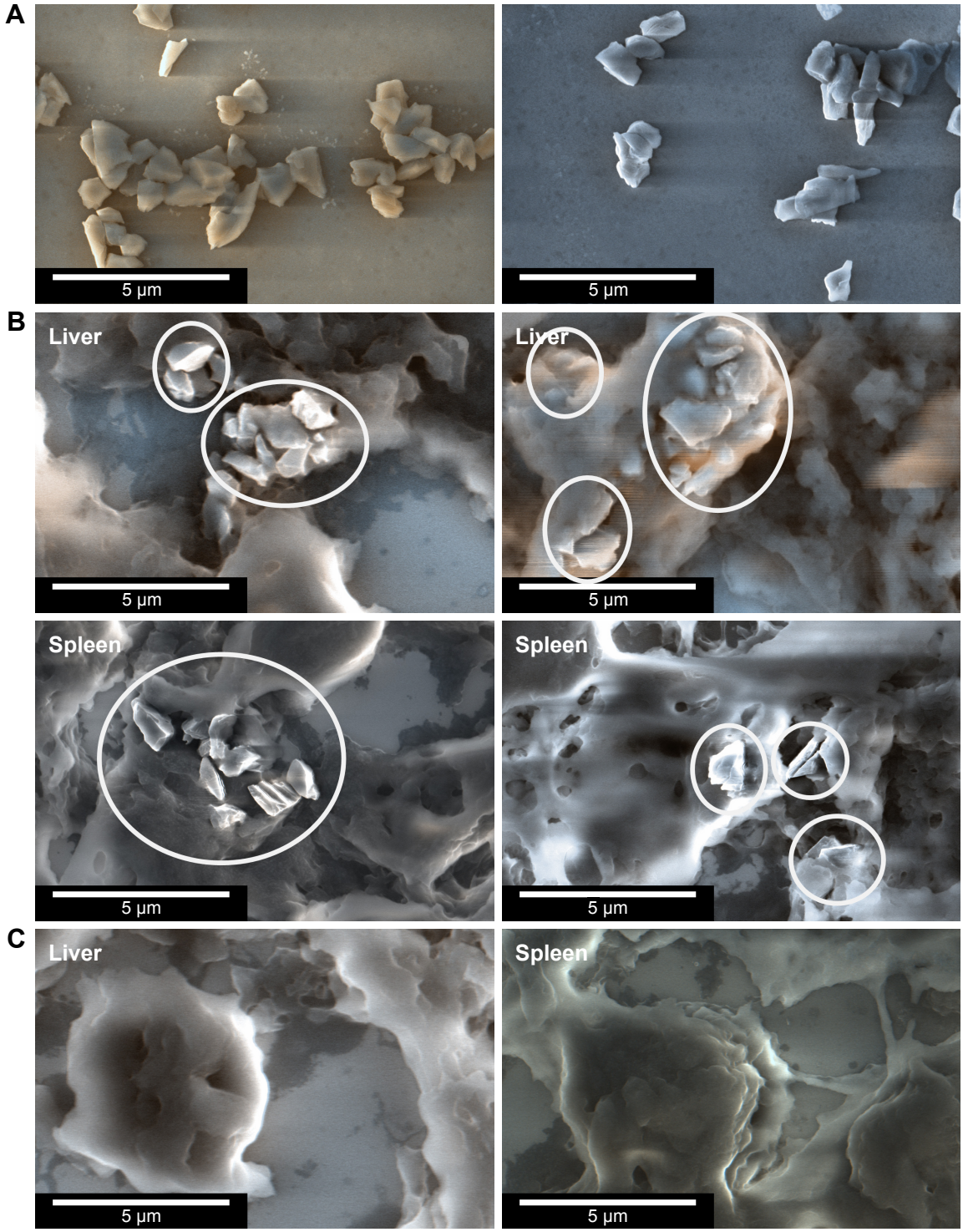

Figure 8 SEM micrographs of FNDP localized in liver and spleen tissues.
Notes: (**A**) Images FNDP-(NV) alone analyzed before injection into animals. (**B**) Images of paraffin sections of liver and spleen tissues dissected from rats treated with FNDP-(NV) in the 14-day study, showing assembly of FNDP-(NV) into the tissue (marked with white circles). (**C**) Images of paraffin sections of liver and spleen tissues dissected from control (PBS-treated) rats.
Abbreviations: FNDP-(NV), fluorescence nanodiamond particles with NV active centers; SEM, scanning electron microscope.

The FNDP-(NV) distribution in our study revealed a preference for accumulation in the liver and spleen, which are generally in accord with reports of bio-distribution of other nanodiamonds and non-NDP injected in vivo in various species and experimental conditions.[29–33] In particular, our data are in accordance with those reported by Purtov et al,[31] where preference of particles deposition in vivo indicated similar distribution to the liver and spleen. Significantly

lesser deposition was noted in in the kidney, heart, and lung. However, the former reference differs from our study by several important attributes: 1) use of radiolabeled BSA (BSA-I^{125}) particles to report on particle localization via autoradiography; 2) smaller particles size (nonfluorescent) of up to 300 nm; 3) species – mice. The former reference carries the advantage of apparent superior sensitivity and quantitation of autoradiography over IVIS and Tecan technology, hence the ability to report and quantify lower loads of particles in the lung, kidney, and heart, even though their dosing regimen was lower (30 mg/kg). It is, however, noteworthy that autoradiography carries caveats such as overestimation of residual free radioligands in tissues.[32]

It is also pertinent to mention the work in rodents (mice and rats) where 100 nm FNDP-(NV)-BSA were tested for similar variables.[34] The latter report also indicated remote distribution from injection site and a lack of mortality. However, it must be noted that the route of FNDP-(NV)-BSA injections was into confined compartments such as intradermal, subcutaneous (at lower doses), or intraperitoneal. While Vaijayanthimala et al[34] also used NIR to detect the local deposition and remote distribution (lymph nodes) of FNDP, their work differs substantially from the present study in respect to particles size, dosing regimens, routes of administration, and variables monitored to assess systemic and local parameters of organ and animal health. Thus, we indeed report unprecedented physiological, biochemical, and PK features for FNDP-(NV)-Z~800.

Inspection of particle deposition in several organs over three time points (acute and subacute) in independent cohorts indicated that the liver burden was 51%, 24%, and 18% of the total infused dose at 90 minutes, 5 days, and 14 days post-infusion, respectively. These temporal changes were mainly noted in the liver and to a lesser extent in the spleen. This observation suggests apparent mechanism(s) by which acute loading of the particles changes over time, possibly by elimination and/or redistribution. The temporal downward trend in organ burden has been alluded to studies in rats where the significant repository of particles in the peritoneum following repeated injection of FNDP-(NV)-BSA (100 nm) was no longer observed in acid digests of the organ 8 weeks postexposure.[34] Distribution of particles from the primary organ of exposure has also been noted following intratracheal application of NDP. In the later study, distribution from the lungs (the primary deposition site by this exposure route) into the systemic circulation was affirmed.[33,35] The mechanism(s) responsible for the apparent temporal changes in our study and the previous report[34] has not been explored in the present study. We speculate that early "noncommitted" presence of particles in the liver and spleen over a short period transitions into a more persistent residency of particles and possibly a permanent depot. Furthermore, hepatic biliary excretion has also been demonstrated with much smaller particles.[36,37] The significance of the dynamic changes of particles storage in the liver and spleen over time should eventually be of significant value in respect to long-term preservation of organ functional integrity and regulatory position on the development path.

Since localization of the particles at the cellular level could not be assessed in solubilized organs (analyzed by Tecan) and whole organ imaging (IVIS) does not carry resolution at the cellular level, we utilized fluorescent microscopy in search of FNDP-(NV) by inspection of 5-µm tissue sections. In the liver (Figure 7), images of single and small particle aggregates were clearly noted in venous sinusoids; yet, adhesion to cells and/or intracellular location cannot be excluded. In fact, Tsoi et al[36] demonstrated the capacity of all liver resident cells (parenchyma, Kupfer cells, and thin endothelial sinusoidal endothelium) to retain nanoparticles. However, these particles were quantum dot composites of up to 100 nm, a marked difference from the FNDP-(NV) used in our studies which average 800 nm. Whether the strain of FNDP-(NV)-Z~800 shares similar distribution and excretion attributes to those in the former reference awaits further studies. In the spleen, where more mature lymphocyte masses mark the "red pulp" and nascent lymphocytes dominate the "white pulp" region, NIR signals were prevalent in the "red pulp" zone as opposed to the "white pulp" zone. The particle distribution in the spleen and liver might represent microvascular disparity as well as the propensity of various indigenous cells to associate with or take up particles. In this context, preliminary studies from our laboratory indicate that FNDP-(NV)-Z~800 incubated in vitro with human umbilical vein endothelial cells do gain access to the intracellular spaces in a concentration- and time-dependent manner (C Marcinkiewicz, unpublished data). Furthermore, intracellular access of FNDP-(NV)-Z~170 has been shown in cultured neurons.[38]

The high, single dose (60 mg/kg by IV injection) used in our safety studies was found to be safe and well tolerated. Safety of high dosage of NDP has been demonstrated with smaller (100 nm) particles in rats.[34] However, the potential for subacute toxicity in prior research was mitigated by the sufficiently low dose in each of the periodic injections rendering the overall "chronic" regimen devoid of adverse structural and/or functional effects in contrast to a single high dose. Our observations are affirmed by the normal hematological and biochemical biomarkers (Figure 4). Such observations could gain credibility considering the number of particles deposited

in the rat liver relative to the high number of hepatocytes (117±30 million cells per gram liver).[39] Considering that 1 mg of FNDP-(NV)-Z~800 contains ~2×10^8 particles (data obtained from ADAMAS Nanotechnologies, as assessed by Malvern DLS [Malvern Instruments, Malvern, UK]), the particle mass found in 1 gram of liver parenchyma (Figure 7, 14-day study) amounts to 4.6×10^7 or ~0.39 particles per cell or one particle in every 2–3 cells on average. If one considers the 800-nm particle a sphere, the volume of a single 800 nm diameter particle amounts to 0.043 μm^3 (calculated by sphere formula). In comparison, the volume of a single hepatocyte (cuboidal dimension of 20 μm diameter) should amount to 8,000 μm^3 and the ratio to the particle volume of 190,000, suggesting that a single intracellular particle would occupy 0.00054% of a single hepatocyte volume. Considering the inert nature of NDP, it is tempting to speculate that the presence of such a limited number of FNDP-(NV) may not suffice to interfere with normal cell function, as monitored by our liver and renal function biomarker tests at least up to 14 days.

Since our technology is developed toward clinical utility where functionalized FNDP-(NV)-Z~800/Bit is intended to interact with platelets, testing the impact of FNDP-(NV) used in the present studies on platelets was of special interest. As demonstrated in Figure 4, platelet count remained normal (both in the 5- and 14-day follow-up studies), as also reported by Moore et al[29] in rat and nonhuman primates (NHP). The latter report is in line with our data, although particles were much smaller (40 nm) and the dosing regimen was also lower (up to 16 mg/kg over 2 weeks vs a single high dose of 60 mg/kg). Of particular interest is the stable platelet count in the NHP study where platelet count remained normal while a 5-month high dosing regimen (25 mg/kg) was sustained. In marked contrast, Kumari et al[40] reported profound platelet activation by nanodiamond functionalized by carboxylation without further BSA blocking steps. These particles (5–10 nm) did activate platelets in mice following systemic exposure, as evident by the aberrant platelet aggregation and TEE. The data from Kumari et al[40] might reflect the nature of the particles, the very high particle number exposure, or lack of the "shielding" effect provided by BSA blocking. However, neither our study nor that reported by Moore et al[29] tracked platelet biology in sufficient detail, an obvious gap that requires further research.

The pilot clearance study with 60 mg/kg particles infusion into anesthetized rats over 30 minutes was designed (Figure 2A) to test the kinetics of particle clearance after treatment. As no precedence for such a study with the specific FNDP-(NV)-Z~800 could be identified, we chose a protocol that stands to avoid potential excessive particles exposure that might lead to adverse events. The dose chosen in our study is expected to induce at the end of the infusion a maximum concentration (C_{max}) of 1 mg/mL of blood (or 2 mg/mL of plasma) if the particles remain in systemic circulation throughout the length of the infusion. Compared to this theoretical C_{max}, the average particle concentration of 58 μg/mL in the blood sample withdrawn immediately post-infusion indicates ~94% elimination of the particles from the systemic circulation within the infusion period. This disparity suggests a rapid elimination rate of 50% clearance every 6 minutes during the infusion period. This calculated $T_{1/2}(\alpha)$ (first elimination time) underwrites the compartmental analysis[35] depicted in Figure 2B. Elucidation of the earlier clearance pattern will have to be assessed in the future in search of the acute MTD. The elimination pattern post-infusion is clearly moderated, but the terminal elimination rate has not yet been fully detailed.

Summary

The objective of the present study was to outline key safety and PK attributes of FNDP-(NV)-Z~800 as a bridge study toward formal GLP preclinical development for IND qualifying dossier. The paucity of information the nanodiamond literature offers likely represents reluctance by the research and regulatory community to engage in the development of particles of the size we chose. Safety and tolerability challenges are likely the reason for such limited application development. Our preliminary work with these particles, en route for development as a tool for imaging of vascular blood clots diagnostics, provides new insights into these particular particles. The safety and PK profile (including organ distribution) detailed in these studies should underwrite future toxicological studies over extended periods of time under the Food and Drug Administration guidance.

Acknowledgment

The authors wish to acknowledge the full financial sponsorship by Debina Diagnostics Inc of all studies performed and reported in this publication.

Disclosure

The authors report no conflicts of interest in this work.

References

1. Man HB, Ho D. Nanodiamonds as platforms for biology and medicine. *J Lab Autom*. 2013;18(1):12–18.

2. Shames AI, Smirnov AI, Milikisiyants S, et al. Fluence-dependent evolution of paramagnetic triplet centers in e-beam irradiated microcrystalline Ib type HPHT diamond. *J Phys Chem*. 2017;121(40):22335–22346.
3. Shenderova OA, Ciftan Hens S. Detonation nanodiamond particles processing, modifications and bio-applications. In: Ho D, editor. *Nanodiamonds*. Vol 4. Boston, MA: Springer; 2010:79–116.
4. Mochalin VN, Shenderova O, Ho D, Gogotsi Y. The properties and applications of nanodiamonds. *Nat Nanotechnol*. 2012;7(1):11–23.
5. Kaur R, Badea I. Nanodiamonds as novel nanomaterials for biomedical applications: drug delivery and imaging systems. *Int J Nanomedicine*. 2013;8:203–220.
6. Zhang J, Tang H, Liu Z, Chen B. Effects of major parameters of nanoparticles on their physical and chemical properties and recent application of nanodrug delivery system in targeted chemotherapy. *Int J Nanomedicine*. 2017;12:8483–8493.
7. Perevedentseva E, Lin YC, Jani M, Cheng CL. Biomedical applications of nanodiamonds in imaging and therapy. *Nanomedicine*. 2013;8(12):2041–2060.
8. Igarashi R, Yoshinari Y, Yokota H, et al. Real-time background-free selective imaging of fluorescent nanodiamonds in vivo. *Nano Lett*. 2012;12(11):5726–5732.
9. Ho D. Nanodiamond-based chemotherapy and imaging. *Cancer Treat Res*. 2015;166:85–102.
10. Bhattacharya K, Mukherjee SP, Gallud A, et al. Biological interactions of carbon-based nanomaterials: from coronation to degradation. *Nanomedicine*. 2016;12(2):333–351.
11. Salaam AD, Hwang PT, Poonawalla A, Green HN, Jun HW, Dean D. Nanodiamonds enhance therapeutic efficacy of doxorubicin in treating metastatic hormone-refractory prostate cancer. *Nanotechnology*. 2014;25(42):425103.
12. Wang X, Low XC, Hou W, et al. Epirubicin-adsorbed nanodiamonds kill chemoresistant hepatic cancer stem cells. *ACS Nano*. 2014;8(12):12151–12166.
13. Marcinkiewicz C, Gerstenhaber JA, Sternberg M, Lelkes PI, Feuerstein G. Bitistatin-functionalized fluorescent nanodiamond particles specifically bind to purified human platelet integrin receptor $\alpha_{IIb}\beta_3$ and activated platelets. *Int J Nanomedicine*. 2017;12:3711–3720.
14. Davis ME, Chen ZG, Shin DM. Nanoparticle therapeutics: an emerging treatment modality for cancer. *Nat Rev Drug Discov*. 2008;7(9):771–782.
15. Huang H, Liu M, Jiang R, et al. Facile modification of nanodiamonds with hyperbranched polymers based on supramolecular chemistry and their potential for drug delivery. *J Colloid Interface Sci*. 2018;513:198–204.
16. Mochalin VN, Pentecost A, Li XM, et al. Adsorption of drugs on nanodiamond: toward development of a drug delivery platform. *Mol Pharm*. 2013;10(10):3728–3735.
17. Li X, Shao J, Qin Y, Shao C, Zheng T, Ye L. TAT-conjugated nanodiamond for the enhanced delivery of doxorubicin. *J Mater Chem*. 2011;21(22):7966–7973.
18. Pham NB, Ho TT, Nguyen GT, et al. Nanodiamond enhances immune responses in mice against recombinant HA/H7N9 protein. *J Nanobiotechnology*. 2017;15(1):69.
19. Zhang Y, Cui Z, Kong H, et al. One-shot immunomodulatory nanodiamond agents for cancer immunotherapy. *Adv Mater*. 2016;28(14):2699–2708.
20. Eidi H, David MO, Crépeaux G, et al. Fluorescent nanodiamonds as a relevant tag for the assessment of alum adjuvant particle biodisposition. *BMC Med*. 2015;13:144.
21. Haziza S, Mohan N, Loe-Mie Y, et al. Fluorescent nanodiamond tracking reveals intraneuronal transport abnormalities induced by brain-disease-related genetic risk factors. *Nat Nanotechnol*. 2017;12(4):322–328.
22. Rosenholm JM, Vlasov II, Burikov SA, Dolenko TA, Shenderova OA. Nanodiamond-based composite structures for biomedical imaging and drug delivery. *J Nanosci Nanotechnol*. 2015;15(2):959–971.
23. Moore LK, Chow EK, Osawa E, Bishop JM, Ho D. Diamond-lipid hybrids enhance chemotherapeutic tolerance and mediate tumor regression. *Adv Mater*. 2013;25(26):3532–3541.
24. Reineck P, Francis A, Orth A, et al. Brightness and photostability of emerging red and near-IR fluorescent nanomaterials for bioimaging. *Adv Opt Mater*. 2016;4(10):1549–1557.
25. Gerstenhaber JA, Barone FC, Marcinkiewicz C, et al. Vascular thrombus imaging in vivo via near-infrared fluorescent nanodiamond particles bioengineered with the disintegrin bitistatin (part II). *Int J Nanomedicine*. 2017;12:8471–8482.
26. Ventresca EM, Lecht S, Jakubowski P, et al. Association of p75(NTR) and α9β1 integrin modulates NGF-dependent cellular responses. *Cell Signal*. 2015;27(6):1225–1236.
27. Zhou J, Li J, Rosenbaum DM, et al. The prolyl 4-hydroxylase inhibitor GSK360A decreases post-stroke brain injury and sensory, motor, and cognitive behavioral deficits. *PLoS One*. 2017;12(9):e0184049.
28. Zhou J, Zhuang J, Li J, et al. Long-term post-stroke changes include myelin loss, specific deficits in sensory and motor behaviors and complex cognitive impairment detected using active place avoidance. *PLoS One*. 2013;8(3):e507503.
29. Moore L, Yang J, Lan TT, et al. Biocompatibility assessment of detonation nanodiamond in non-human primates and rats using histological, hematologic, and urine analysis. *ACS Nano*. 2016;10(8):7385–7400.
30. Rojas S, Gispert JD, Martín R, et al. Biodistribution of amino-functionalized diamond nanoparticles. In vivo studies based on 18F radionuclide emission. *ACS Nano*. 2011;5(7):5552–5559.
31. Purtov K, Petunin A, Inzhevatkin E, et al. Biodistribution of different sized nanodiamonds in mice. *J Nanosci Nanotechnol*. 2015;15(2):1070–1075.
32. Lidow MS, Goldman-Rakic PS, Rakic P, Gallager DW. Differential quenching and limits of resolution in autoradiograms of brain tissue labeled with 3H-, 125I- and 14C-compounds. *Brain Res*. 1988;459(1):105–119.
33. Miller MR, Raftis JB, Langrish JP, et al. Inhaled nanoparticles accumulate at sites of vascular disease. *ACS Nano*. 2017;11(5):4542–4552.
34. Vaijayanthimala V, Cheng PY, Yeh SH, et al. The long-term stability and biocompatibility of fluorescent nanodiamond as an in vivo contrast agent. *Biomaterials*. 2012;33(31):7794–7802.
35. Zhang X, Yin J, Kang C, et al. Biodistribution and toxicity of nanodiamonds in mice after intratracheal instillation. *Toxicol Lett*. 2010;198(2):237–243.
36. Tsoi KM, Macparland SA, Ma XZ, et al. Mechanism of hard-nanomaterial clearance by the liver. *Nat Mater*. 2016;15(11):1212–1221.
37. Zhang YN, Poon W, Tavares AJ, Mcgilvray ID, Chan WCW. Nanoparticle-liver interactions: cellular uptake and hepatobiliary elimination. *J Control Release*. 2016;240:332–348.
38. Simpson DA, Morrisroe E, Mccoey JM, et al. Non-neurotoxic nanodiamond probes for intraneuronal temperature mapping. *ACS Nano*. 2017;11(12):12077–12086.
39. Sohlenius-Sternbeck AK. Determination of the hepatocellularity number for human, dog, rabbit, rat and mouse livers from protein concentration measurements. *Toxicol In Vitro*. 2006;20(8):1582–1586.
40. Kumari S, Singh MK, Singh SK, Grácio JJ, Dash D. Nanodiamonds activate blood platelets and induce thromboembolism. *Nanomedicine*. 2014;9(3):427–440.
41. Woo HN, Chung HK, Ju EJ, et al. Preclinical evaluation of injectable sirolimus formulated with polymeric nanoparticle for cancer therapy. *Int J Nanomedicine*. 2012;7:2197–2208.

Supplementary materials

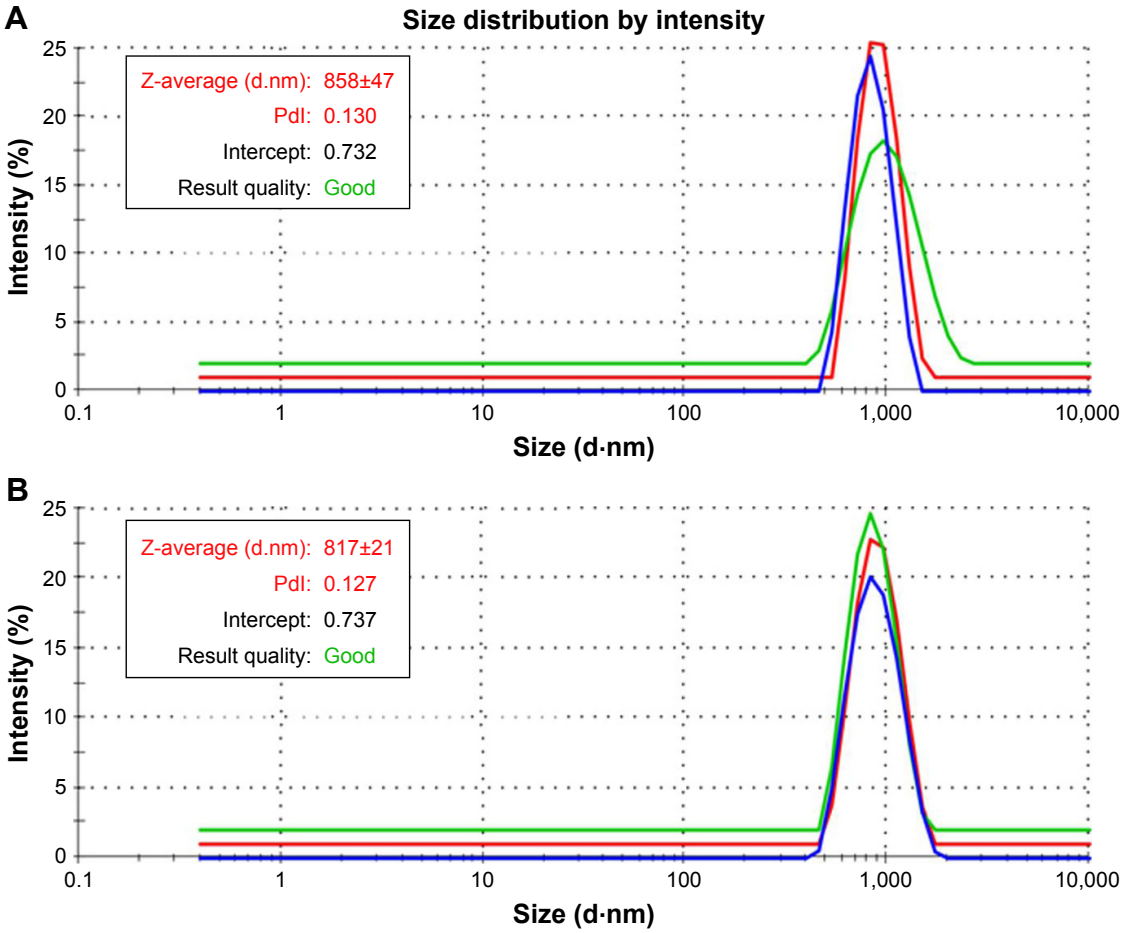

Figure S1 Dynamic light scattering size distribution of FNDP-(NV) in the aqueous suspension.
Notes: FNDP measured (**A**) after blocking with BSA and (**B**) before blocking with BSA. Samples were measured in three repeats superimposed in each graph. Z-average values are presented as mean±SD.
Abbreviations: FNDP-(NV), fluorescence nanodiamond particles with NV active centers; d.nm, diameter in nanometers; PdI, polydispersity index.

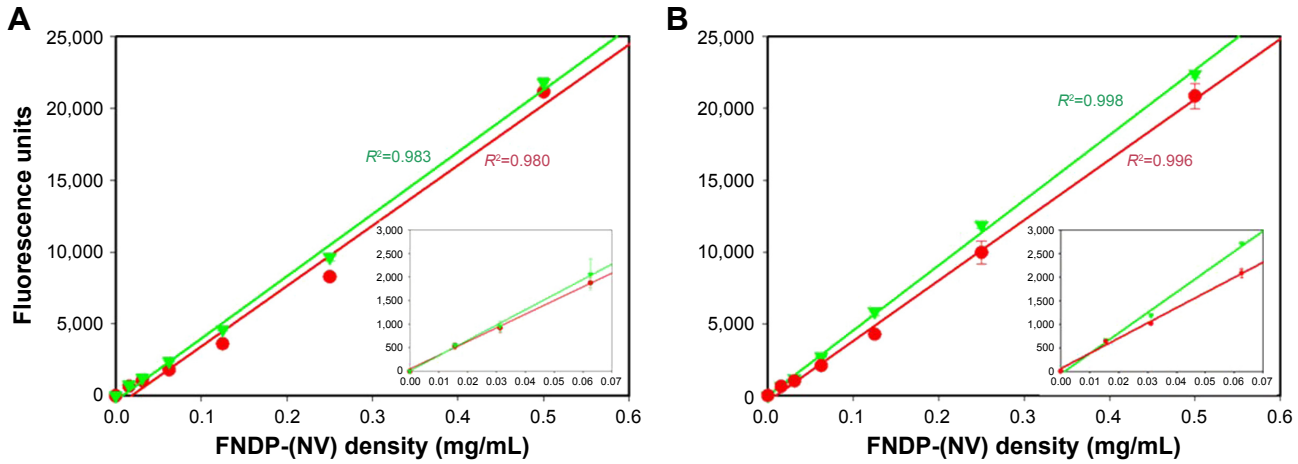

Figure S2 Comparison of standard curves prepared from FNDP-(NV) in water vs rat liver tissue or blood followed by acid solubilization and centrifugal extraction.
Notes: Regression plots of standard curve prepared in water (triangles/green) and processed together with (**A**) liver tissue by treatment with 12 N HCl (circles/red) for organ distribution study and (**B**) blood by treatment with 12 N HCl (circles/red) for PK study. Error bars represent SD from quadruplicate determinations. Insets in the plots show extension of the scale for lower densities of FNDP-(NV).
Abbreviations: FNDP-(NV), fluorescence nanodiamond particles with NV active centers; PK, pharmacokinetic.

Table S1 Summary of neurobehavioral tests results for each individual animal in the 5- and 14-day study

	PBS				FNDP			
5-day study								
mNSS								
Day 0	0	0	0		0	0	0	0
Day 1	0	0	0		0	0	0	0
Day 5	0	0	0		0	0	0	0
Foot fault (%)								
Day 0	0/24	0/33	0/30		0/34	0/41	0/38	0/48
Day 1	0/52	0/59	0/67		0/20	0/15	0/34	0/14
Day 5	0/48	0/54	0/33		0/50	0/47	0/48	0/36
Hind limb								
Day 0	0	0	0		0	0	0	0
Day 1	0	0	0		0	0	0	0
Day 5	0	0	0		0	0	0	0
Beam balance								
Day 0	0	0	0		0	0	0	0
Day 1	0	0	0		0	0	0	0
Day 5	0	0	0		0	0	0	0
Self-suspension time (seconds)								
Day 0	6	7	8		8	10	9	10
Day 1	8	7	10		14	12	15	12
Day 5	9	8	9		13	13	15	14
Angle of increase (degrees)								
Day 0	35	35	35		35	35	35	35
Day 1	35	35	35		35	35	35	35
Day 5	35	35	35		35	35	35	35
14-day study								
mNSS								
Day 0	0	0	0	0	0	0	0	0
Day 1	0	0	0	0	0	0	0	0
Day 7	0	0	0	0	0	0	0	0
Day 14	0	0	0	0	0	0	0	0
Foot fault (%)								
Day 0	0/33	0/40	0/51	0/32	0/30	0/27	0/33	0/32
Day 1	0/21	0/30	0/27	0/22	0/22	0/20	0/14	0/20
Day 7	0/61	0/63	0/66	0/57	0/38	0/51	0/40	0/28
Day 14	0/54	0/55	0/50	0/57	0/47	0/38	0/38	0/41
Hind limb								
Day 0	0	0	0	0	0	0	0	0
Day 1	0	0	0	0	0	0	0	0
Day 7	0	0	0	0	0	0	0	0
Day 14	0	0	0	0	0	0	0	0
Beam balance								
Day 0	0	0	0	0	0	0	0	0
Day 1	0	0	0	0	0	0	0	0
Day 7	0	0	0	0	0	0	0	0
Day 14	0	0	0	0	0	0	0	0
Self-suspension time (seconds)								
Day 0	8	8	8	9	9	10	10	10
Day 1	7	7	7	7	12	17	11	20
Day 7	9	10	10	9	18	20	25	27
Day 14	10	10	10	10	19	18	20	18
Angle of increase (degrees)								
Day 0	35	35	35	35	35	35	35	35
Day 1	35	35	35	35	35	35	35	35
Day 7	35	35	35	35	35	35	35	35
Day 14	35	35	35	35	35	35	35	35

Abbreviations: FNDP, fluorescence nanodiamond particles; mNSS, modified neurologic severity score.

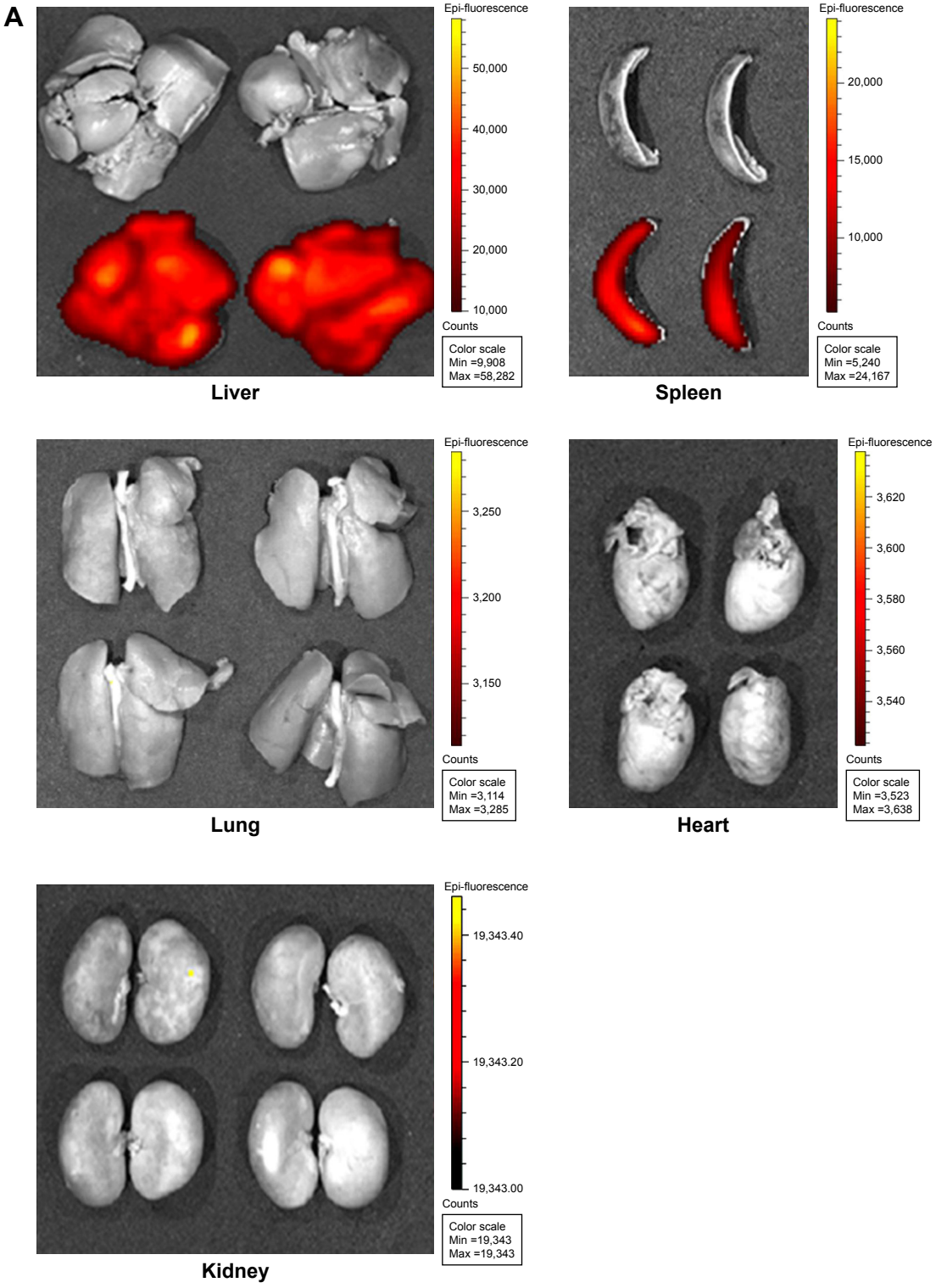

Figure S3 (*Continued*)

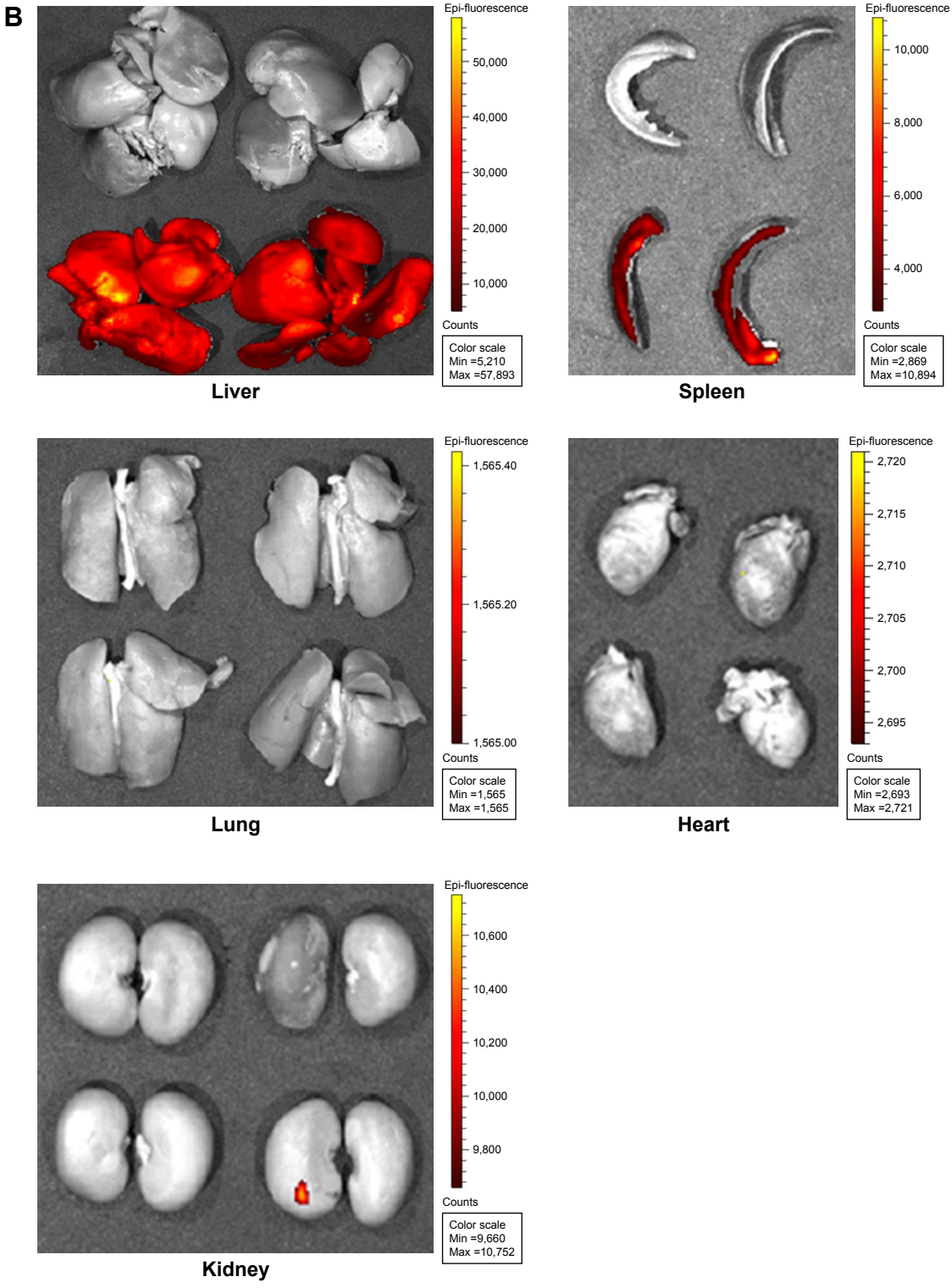

Figure S3 Representative IVIS images of dissected, isolated intact organs of rats.
Notes: (**A**) 5-day study; (**B**) 14-day study. Organs obtained from two control animals (injected with PBS) are presented on the top row of each image, whereas organs obtained from animals treated with FNDP-(NV) are presented on the bottom row of each image. Intensity of fluorescence is in red (low) to yellow (high) color scale.
Abbreviations: FNDP-(NV), fluorescence nanodiamond particles with NV active centers; IVIS, in vivo imaging system.

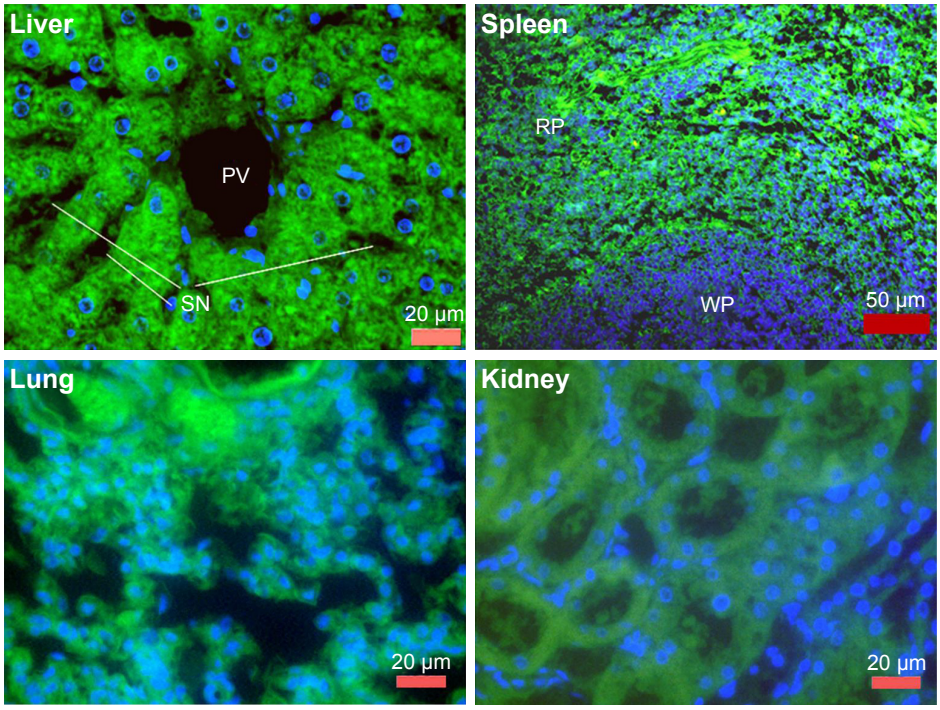

Figure S4 Fluorescence microscopy images of paraffin sections of liver, spleen, lung, and kidney for control rats treated with vehicle (PBS), obtained from the 14-day study.
Notes: Tissue slides were stained with FITC-phalloidin (green) and DAPI (blue). Images were taken under a fluorescence microscope (Olympus FSX100) with 400× magnification for liver, lung, and kidney, and 200× for spleen magnifications.
Abbreviations: FITC, fluorescein isothiocyanate; PV, portal vein; SN, sinusoids; RP, red pulp; WP, white pulp.

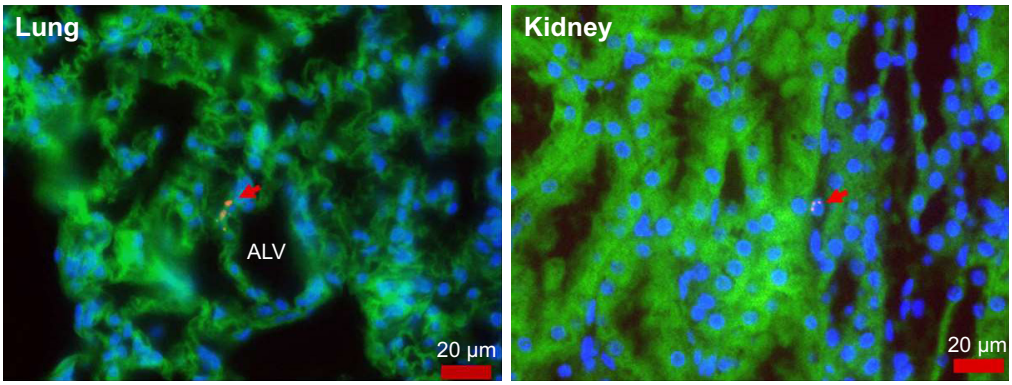

Figure S5 Fluorescence microscope images of paraffin sections of lung and kidney of rats treated with FNDP-(NV), collected on postinjection day 14.
Notes: Tissue slides were stained with FITC-phalloidin (green) and DAPI (blue). FNDP are in yellow/red (TRITC filter). Images were taken under a fluorescence microscope (Olympus FSX100) with 400× magnification. Red arrows indicate localization of FNDP-(NV) in single points of tissues.
Abbreviations: FNDP-(NV), fluorescence nanodiamond particles with NV active centers; FITC, fluorescein isothiocyanate; TRITC, tetramethylrhodamine isothiocyanate; ALV, alveoli.